# ANALYSIS OF THE CHARACTERISTICS ABOUT GYEONG-GANG FAULT ZONE THROUGH REMOTE SENSING TECHNIQUES

Jin-kyong Hwang, Jong-kuk Choi and Joong-sun Won

Department of Earth System Science, Yonsei University
E-mail: eastlife@yonsei.ac.kr

**ABSTRACT:** Lineament is defined generally as a linear feature or pattern on interpretation of a satellite image and indicates the geological structures such as faults and fractures. For this reason, a lineament extraction and analysis using remote sensing images have been widely used for mapping large areas. The Gyeong-gang Fault is a NNE trending structure located in Gangwon-do and Kyeonggi-do district. However, a few geological researches on that fault have been carried out and its trace or continuity is ambiguous. In this study, we investigate the geologic features at Gyeong-gang Fault Zone using LANDSAT ETM+ satellite image and SRTM digital elevation model. In order to extract the characteristics of geologic features effectively, we transform the LANDSAT ETM+ image using Principal Component Analysis (PCA) and create a shade relief from SRTM data with various illumination angles. The results show that it is possible to identify the dimensions and orientations of the geologic features at Gyeong-gang Fault Zone using remote sensing data. An aerial photograph interpretation and a field work will be future tasks for more accurate analysis in this area.

**KEY WORDS:** Lineament, Gyeong-gang Fault, LANDSAT ETM+, SRTM, Principal Component Analysis

## 1. INTRODUCTION

Remote sensing data have been widely used for recognizing geological structures due to its large-area or synoptic coverage which enables the detection of regional geological features. Especially, lineament analysis using remote sensing data is a valuable source of information for studying the structural setting. In the geological point of view, the lineaments are usually faults, joints, or stratigraphic boundaries. Topographic characteristics might be indicators of the surface expression of geologic deformation.

Korean Peninsula has experienced a series of diastrophisms to yield a complicated structures and most ground surface is covered with alluvium or vegetation so that these geological and geographical conditions limit the applications of remote sensing to geologic interpretation. However, it is possible to extract useful information of geologic structures and lithologic discrimination of different rock units through various data and image processing.

The Gyeong-gang Fault is a NNE trending structure located in Gangwon-do and Kyeonggi-do district. The fault zone is covered with alluvium so that it makes hard to identify its trace or continuity.

This study is aimed at identifying the dimensions and orientations of geologic features around Gyeong-gang Fault Zone using remote sensing data. LANDSAT ETM+ satellite image and Shuttle Radar Topography Mission (SRTM) digital elevation model (DEM) were used. In order to extract the geologic features effectively, Principal Component Analysis (PCA) and a shade relief map from SRTM were used.

## 2. GEOLOGIC SETTING OF THE STUDY AERA

The Korean Peninsula is near the south-eastern margin of the Eurasian plate and consists of three Precambrian massifs, two Phanerozoic orogenic belts, two Palaeozoic and one Cretaceous sedimentary basins (Fig. 1 (a), Ree et al., 2003). The Kyeonggi massif is composed primarily of basement gneisses and schists together with overlying supracrustal rocks (Fig. 1 (b)). These metamorphic rocks have experienced multiple deformation and poly-metamorphism. The Kyeonggi massif has been regarded as an eastern promontory of the South China craton, and the Nangrim and Yongnam massifs have been regarded as parts of the Sino-Korean craton. Hence, both northern and southern margins of the Kyeonggi massif are considered as tectonic boundaries (Lee and Cho, 2008).

The Gyeong-gang Fault was inferred to be a product of large scale crustal block movement which took place in Korea and named Gyeong-gang Thrust Fault by Kim (1973). Mylonitic chlorite schist is exposed along Gyeong-gang Fault at Cheongpyeong and Yangsuri. It is considered that the fault was a northeast trending thrust and it was formed during the Proterozoic era (Kim et al., 1981). However, the dextral strike-slip displacements of Gyeong-gang Fault are found at Chuncheon and Hwacheon (Lee et al., 1974; Park et al., 1997).

The geological characteristics of Gyeong-gang Fault Zone are poorly understood because not only the alluvium is extensive in this area but also a few geological researches on that fault have been carried out. Therefore, more comprehensive studies on the Gyeong-gang Fault Zone are required.

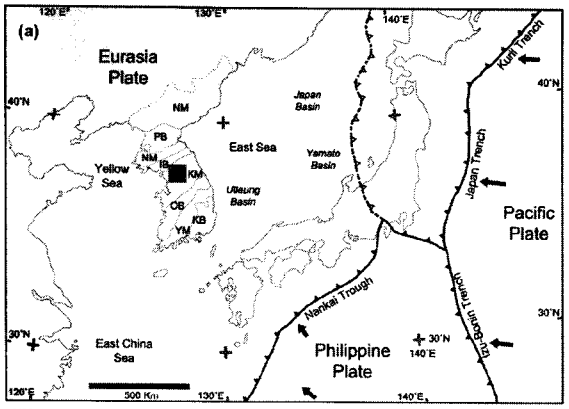


NM: Nangrim Massif, PB: Pyongnam Basin, IB: Imjingang Belt, KM: Kyeonggi Massif
OB: Okchon Belt, YM: Yongnam Massif, KB: Kyeongsang Basin ■ : study area.

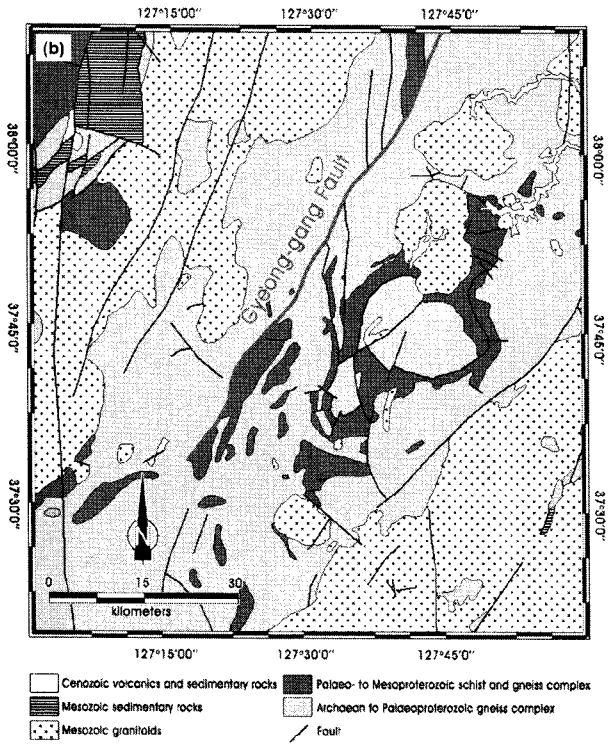


Figure 1. (a) Current tectonic map of East Asia (Ree et al., 2003). (b) A simplified geological map of the study area.

## 3. DATA PROCESSING AND RESULTS

In this study, Landsat ETM+ data was used to detect geological units and lineaments around Gyeong-gang Fault Zone. Fig. 2 shows that many northeast trending lineaments are developed in the whole study area. Compared with the geological map in Fig. 1 (b), in Fig. 2 the lineaments indicate fairly well the geologic features such as faults and rock units. However, the Gyeong-gang Fault does not appear as a prominent topographic feature in the image compared with other faults. In order to extract the geologic features effectively, we carried out a PCA for the image, which removes redundant information from visible and near-infrared (NIR) multi-spectral data. The Principal Component Transform (PCT) of the raw remote sensing data can result in new principal component images that may be more interpretable than the original data (Jensen, 1996; Nama, 2004). It is well know the first component of PCA largely reflects the topographic effects rendered in a multi-spectral image.


Figure 2. The Landsat ETM+ image (true color composite of bands 3, 2, 1 by R, G, B) of the study area.

Table 1 shows the statistics of the 6 principal components resulted from the 6 ETM+ bands (1-5 and 7). The eigen value indicates amount of information that each PC has. The magnitude and sign of eigenvector loadings give an indication of which spectral properties from vegetation, rocks and soil are responsible for the statistical variance (Yésou et al., 1993, 1994).

PC1 of the ETM+ image accounts for 71.9% of the variance in the entire multi-spectral data, and PC2 accounts for 23.1% of the remaining variance. Cumulatively, these two components account for 95.0% of the variance.

In the PC1 image, band 1, 2, 3 showed the higher contribution in terms of factor loading than other bands. Therefore, the PC1 image is useful for classification of vegetation, and surface lineament covered by vegetation can be mapped by PC1. In the PC2 image NIR bands 4 and 5 had positive factor loading values, so it is expected that soil and water show high reflectance and appear as the bright pixels in the NIR bands. It means that PC2 image provides discrimination between erosional and depositional terrains owing to the relative properties according to their lithology, weathering and erosional characteristics. For instance, a part of the Mesozoic granitoids can be distinguished from gneiss complexes in PC2 image (Fig. 3). In short, PC1 and PC2 are most effective to reveal the geologic features about Gyeong-gang Fault Zone: PC1 is effective for structural and

morphologic studies while PC2 is good for rock type discrimination.

Table 1. The PCA results using the 6 ETM+ bands (1-5 and 7).

| (a) Eigenvalues | | | | | | |
|---|---|---|---|---|---|---|
| PCs | PC1 | PC2 | PC3 | PC4 | PC5 | PC6 |
| values | 10010.6 | 3222.8 | 478.6 | 130.0 | 44.3 | 40.4 |
| % | 71.88 | 23.14 | 3.44 | 0.93 | 0.32 | 0.29 |
| (b) Eigenvectors | | | | | | |
| Band | PC1 | PC2 | PC3 | PC4 | PC5 | PC6 |
| 1 | 0.47 | -0.16 | -0.31 | -0.80 | -0.09 | 0.08 |
| 2 | 0.47 | -0.03 | -0.36 | 0.34 | 0.10 | -0.72 |
| 3 | 0.52 | -0.13 | -0.19 | 0.49 | -0.17 | 0.64 |
| 4 | -0.08 | 0.82 | -0.49 | -0.03 | 0.23 | 0.17 |
| 5 | 0.29 | 0.5 | 0.42 | -0.03 | -0.68 | -0.16 |
| 7 | 0.25 | 0.18 | 0.57 | -0.06 | 0.66 | 0.07 |
| (c) Degree of Correlation | | | | | | |
| Band | PC1 | PC2 | PC3 | PC4 | PC5 | PC6 |
| 1 | 0.96 | -0.18 | -0.14 | -0.19 | -0.01 | 0.01 |
| 2 | 0.98 | -0.04 | -0.16 | 0.08 | 0.01 | -0.09 |
| 3 | 0.98 | -0.14 | -0.08 | 0.11 | -0.02 | 0.08 |
| 4 | -0.16 | 0.96 | -0.22 | -0.01 | 0.03 | 0.02 |
| 5 | 0.69 | 0.68 | 0.22 | -0.01 | -0.11 | -0.02 |
| 7 | 0.64 | 0.21 | 0.26 | -0.01 | 0.09 | 0.01 |

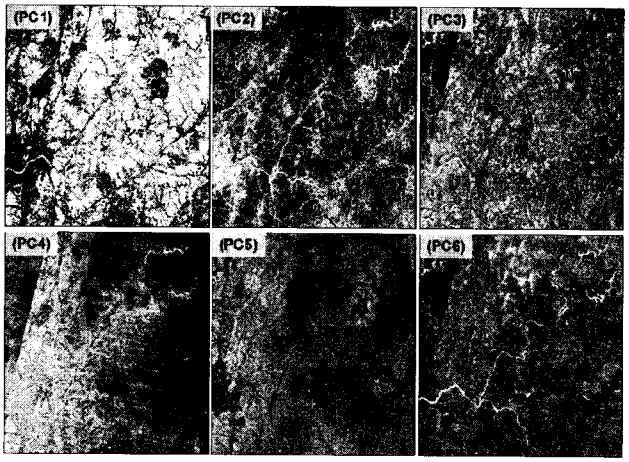


Figure 3. Principal component images of the study area from the LANDSAT ETM+. The dashed line (PC2) represents rock boundaries (inferred).

SRTM DEM with a 90 m spatial resolution was also used for detecting lineaments in the study area because lineaments can be distorted by human interference or vegetation on LANDSAT ETM+ image can be detected on DEM as topographic features.

Shaded relief images from digital elevation model are alternatives to low sun-angle satellite image using artificial illumination sources from various angles (Zhou, 1992). We created 9 shaded relief images from various angles, because the pattern of detected lineament from shaded relief is slightly changed under different illumination conditions (Fig. 4). Altitude 90 means the light source is directly overhead.

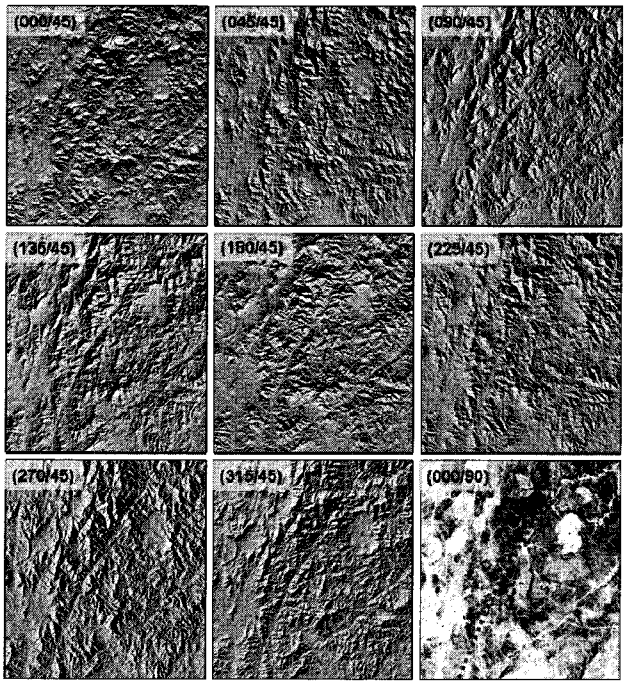


Figure 4. Shaded relief images under various illumination conditions (Azimuth/Altitude). The dashed line represents an inferred lineament as an extension of the Gyeong-gang Fault.

In Fig. 4, the shaded relief image from altitude 90 indicates erosional terrains or artificially developed area and the Gyeong-gang Fault appears as a dominant lineament with NE trend. Especially, topographic feature which was not revealed on LANDSAT ETM+ image is detected at both ends of the fault and it can be considered as a southern extension of Gyeong-gang Fault.

A total of 129 dominant lineaments were traced along Gyeong-gang Fault Zone from the principal component images and shaded relief images.

The map of lineament with its frequency distribution and orientation is shown in Fig. 5. The blue line represents the lineament that corresponds to Gyeong-gang Fault and a total length of the lineament is about 98.1km (Fig. 5 (a)). A total of 72 lineaments are less than 10 km in length and the maximum length is 50.3km (Fig. 5 (b)). Orientation of lineaments is plotted as length-weighted and frequency-weighted rose-diagrams to identify the significant trend. These two rose-diagrams showed great similarities as being concentrated in N40W and N50E directions (Fig. 5 (c)).

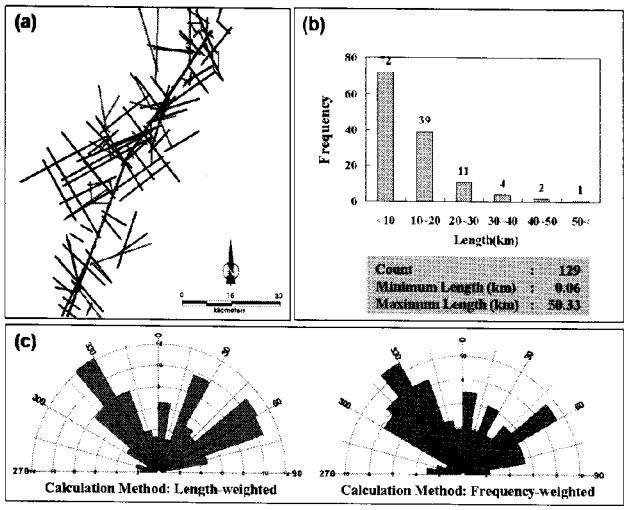


Figure 5. Lineament analysis: (a) Lineament map (red line: extracted lineaments from PC images, black line: extracted lineaments from shaded relief images, blue line: lineament inferred as Gyeong-gang Fault; (b) frequency distribution of lineaments; and (c) rose-diagrams of the lineaments.

## 4. CONCLUSIONS

The conclusions drawn from this study are as follows:

1) From the result of PCA, the PC1 image was effective for studying topographic effects and surface lineaments covered with vegetation.

2) The PC2 was highly correlated with band 4 and 5 and was effective for soil and water classification. It implies that PC2 image provides useful information about the relative properties according to their lithology, weathering and erosional characteristics in the study area.

3) The shaded relief images from DEM were useful for detecting the topographic features which had not been revealed on LANDSAT ETM+ image due to artificial features or vegetations. However, cautions must be taken for interpreting lineament because it is largely affected by illumination angles.

4) We have extracted geological lineaments along Gyeong-gang Fault Zone effectively using remote sensing data. Further, analysis of these lineaments greatly improved the understanding of the characteristics about Gyeong-gang Fault Zone. The obtained lineaments are to be used for field study and validation.

This study showed that it is possible to identify and trace the Gyeong-gang Fault Zone. For more accurate analysis, an aerial photograph interpretation and a field work are needed in the future.

## REFERENCES

Cho, M., Kim, H., Lee, Y., Horie, K. and Hidaka, H., 2008. The oldest (ca. 2.51 Ga) rock in South Korea: U-Pb zircon age of a tonalitic migmatite, Daeijak Island, western Gyeonggi massif. *Geosciences Journal*, 12(1), pp. 1-6.

Jensen, J., 1996. *Introductory digital image processing: A remote sensing perspective, 2ed.* Prentice Hall, New Jersey, pp. 172-179.

Kim, J., Park, S. and Lee, B., 1981. Explanatory text of the geological map of Chengpyeng sheet. Korea Institute of Energy and Resources.

Kim, O., 1973. The stratigraphy and structure of the metamorphic complex in the northwestern area of Kyonggi massif. *The Journal of the Korean Institute of Mining Geology,* 6(4), pp. 201-208.

Lee, D., Lee, H., Nam, K. and Yang, S., 1974. Explanatory text of the geological map of Chuncheon sheet. Korea Institute of Energy and Resources.

Nama, E., 2004. Lineament detection on Mount Camerron during the 1999 volcanic eruptions using Landsat ETM. *International Journal of Remote Sensing,* 25(3), pp. 501-510.

Park, K., Lee, B., Cho, D. and Kim, C., 1997. Geologic Report of the Hwacheon Sheet. Korea Institute of Energy and Resources.

Ree, J., Lee, Y., Rhodes, E., Park, Y., Kwon, S., Chwae, U., Jeon, J. and Lee, B., 2003. Quaternary reactivation of Tertiary faults in the southeastern Korean Peninsula: Age constraint by optically stimulated luminescence dating. *The Island Arc,* 12, pp. 1-12.

Yésou, H., Besnus, Y. and Rolet, J., 1993. Extraction of spectral information from Landsat TM data and merger with SPOT panchromatic imagery. *ISPRS Journal of Photogrammetry and Remote Sensing,* 48, pp. 23-36.

Yésou, H., Besnus, Y. and Rolet, J., 1994. Perception of geological body using multi source remotely-sensed data. *International Journal of Remote Sensing,* 15, pp. 2495-2510.

Zhou, Q., 1992. Relief shading using digital elevation models. *Computers & Geosciences,* 18(8), pp. 1035-1045.